Acta Cryst. (1980). A**36**, 947–951

'White Beam' Synchrotron X-ray Interferometry

BY M. HART

Wheatstone Laboratory, King's College, Strand, London WC2R 2LS, England

M. SAUVAGE

LURE, Bâtiment 209C, Université Paris-Sud, 91405 Orsay CEDEX, France

AND D. P. SIDDONS

Wheatstone Laboratory, King's College, Strand, London WC2R 2LS, England

(*Received* 12 *February* 1980; *accepted* 18 *May* 1980)

Abstract

The first successful moiré topography using the 'white beam' of synchrotron radiation from the DCI storage ring is reported. Moiré X-ray topography is applied in order to study in quantitative detail the beam heating which inevitably occurs at powerful storage-ring sources. The maximum temperature rise observed was 1·39 K and several ways of reducing the thermal load are examined in detail. Schemes for the implementation of high-resolution interferometric spectroscopy and the criteria of elastic and thermal design are discussed.

1. Introduction

The use of X-ray interferometers with synchrotron radiation has so far been restricted to multiple-crystal arrangements (Bonse & Materlik, 1976; Bonse, Spieker, Hein & Materlik, 1979). Whilst such arrangements have advantages when combined with photographic detection, they have several disadvantages compared with monolithic scanning interferometers when used with photon counting techniques. We describe here some experiments made with a silicon interferometer on the DCI storage ring at Orsay, France, to determine the conditions under which X-ray interferometers might be used in the white beam of a synchrotron radiation source. We show that, for wavelengths shorter than that of the peak in the power spectrum of the storage ring (λ_{max} is 1·53 Å for DCI when running at 1·72 GeV), it is possible to provide beam conditions which will saturate most photon counters, whilst not introducing unacceptably large thermal strains in the interferometer. We also show that the thermal strain introduced into the silicon interferometer is mainly determined by the total beam power incident on the crystal, and that the spatial distribution of the absorbed power within the beam has very little effect on the resultant strain pattern.

The interferometer used in these experiments is shown in Fig. 1. It is of the rigid Laue-case type, the thickness of each of the three wafers being about 0·5 mm. The distance between the first and last wafers is 25 mm. With these dimensions a beam cross section of 6 × 12 mm is possible at a wavelength of 1 Å. Larger beam cross sections would cause the non-interfering and interfering beams to overlap. In practice, energy-resolving photon counters such as scintillation counters or semiconductor detectors are saturated when the beam size is approximately 1 × 1 mm. Since in interferometric spectroscopy one would wish to use finely collimated beams so as to achieve high energy resolution, we have studied in detail the influence of beam area on interferometer performance.

2. White-beam moiré patterns

The beam conditions at DCI were 1·72 GeV and 230 ± 30 mA throughout the experiments. Fig. 2(*a*) shows

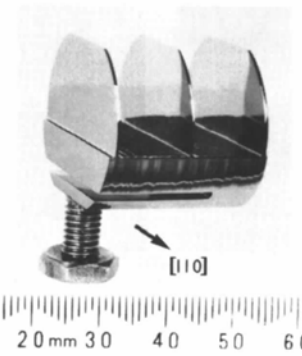

Fig. 1. Monolithic silicon interferometer with strain and thermal isolation of the mounting region.

0567-7394/80/060947-05$01.00

the interference pattern when the interferometer is exposed to the direct white beam, arranged for dispersion in the vertical plane. The beam cross section was 6 × 11 mm and we calculate that the total power dissipation in the first wafer of the interferometer is 1·04 W. Even with this amount of power, moiré fringes can still be seen so that moiré topography is as straightforward as in the laboratory. The apparent lack of contrast on the right of the photograph is due to geometrical resolution effects (the source size of DCI is rather large and the distance between the interferometer and film was about 200 mm). The pattern observed is easily interpreted as a dilation moiré pattern with a smoothly varying dilation over the width of the image. This is expected since the base of the interferometer is an efficient heat sink; the temperature of the splitter wafer will be lower near its base than at its free end.

We know that the interferometer is intrinsically strain-free [from topographs taken under isothermal conditions with Mo $K\alpha_1$ radiation in the laboratory (Aldred, 1970)]. We can therefore associate all the strain observed in this image with beam heating, and indeed we can plot differential temperature profiles in the imaged area by simply measuring the fringe spacing in a direction parallel to the plane of diffraction. This tells us *directly* the local strain, and, through the thermal-expansion coefficient, the temperature differential. This approximation is exact if the beam-splitting wafer totally absorbs the incident flux. Calculations of the incident power spectrum and of the power absorption in the interferometer (Fig. 3) show that the approximation is justified and leads to errors of less than 3%. In order to preserve the thermal symmetry of the interferometer and to isolate elastically the diffracting wafers from the inhomogeneous mounting strains a leaf-spring was cut into the silicon base as shown in Fig. 1. Since the base of the interferometer is 6·5 mm thick, its thermal impedance is 4 times less than that of the mounting leaf-spring and 13 times lower than that of the analyser wafer. We therefore expect that the top edge of a uniformly heated wafer will be very much hotter than the bottom edge (where it meets the base) and that the base of the interferometer will be approximately isothermal. Of course, the whole interferometer will equilibrate above ambient temperature and we measure only temperature differences between the beam-splitting wafer and the remainder of the interferometer. Halfway up the analyser in Fig. 2(*a*), *i.e.* 5·5 mm above the interferometer base, the fringe spacing is 54 μm; corresponding to a temperature differential of 1·39 K. With appropriate thermal design one could maximize the thermal impedance of the leaf-spring and so design crystal optical systems which operate above ambient temperature with thermally isotropic diffracting elements.

The longitudinal thermal impedance of a rod is inversely proportional to ab/l, where a and b are its cross-sectional dimensions and l is the length. On the other hand, its stiffness is proportional to Ka^3b/l in torsion and to a^3b/l^3 if bent by a force applied at one end (K is a function of a/b). Hence one can independently control, at the design stage, the thermal and elastic properties of a monolithic X-ray optical system. This design freedom is extremely convenient in practice.

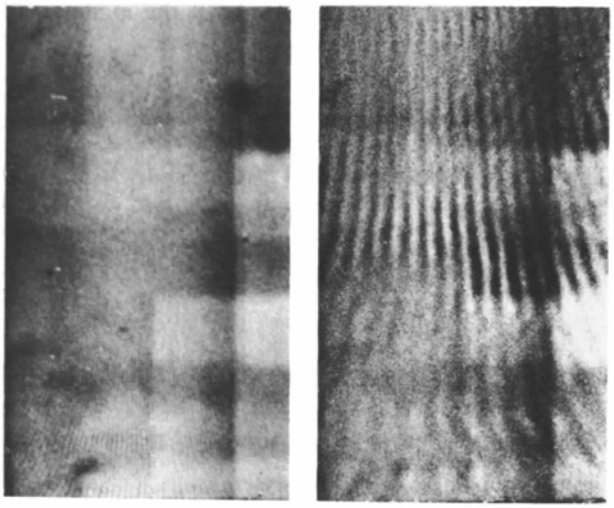

(*a*) (*b*)

Fig. 2. (*a*) White-beam moiré pattern obtained with the 220 Bragg reflection at 1 Å wavelength. (*b*) Similar to (*a*) but with a thin glass thermal filter in front of the interferometer. The base of the interferometer is along the lower edge of the field of view. Field 11 × 6 mm; exposure time 15 s.

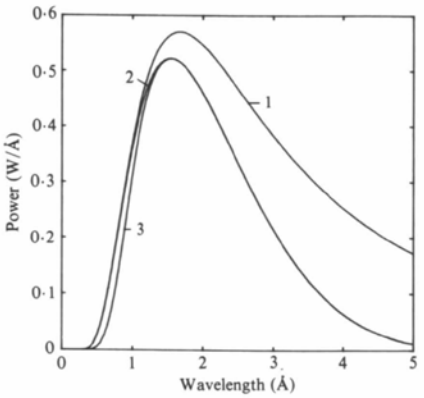

Fig. 3. Power spectra for DCI at 1·72 GeV integrated over ±1·5 × 10^{-4} rad vertically and 5·5 × 10^{-4} rad horizontally. Curve (1) is the intrinsic spectrum, curve (2) shows the spectrum after the beryllium window and curve (3) shows the power spectrum absorbed in the beam splitter of the silicon interferometer.

3. Theoretical power spectrum

Curve (1), Fig. 3, shows the power spectrum produced by the storage ring, calculated according to a formula due to Schwinger (1949) for the conditions prevailing at the time of the experiment (1·72 GeV, 250 mA). Curve (2) of the same figure shows the beam power incident upon the beam splitter after filtration by the beryllium vacuum windows (approximately 325 μm thick) in the beam line. It is difficult to calculate the effect of the windows and the short air path precisely, since the absorption coefficients of Be, O and N are not precisely known. In Fig. 3 the influence of the air has been ignored.

The interferometer splitter wafer has an absorption factor (μt) of 2 at 1 Å. If we take the Victoreen expression for the absorption coefficient of silicon (*International Tables for X-ray Crystallography*, 1968) then the power absorbed by it from the spectrum of Fig. 3, curve (2), is shown in Fig. 3, curve (3). We see that nearly all of the incident power is absorbed by the first wafer of the interferometer. It follows that most of the heat can be absorbed instead in a non-diffracting plate of some suitable material, *e.g.* glass or silicon, chosen to have absorption properties similar to those of the analyser and placed in front of the interferometer. If the non-diffracting plate has an absorption factor of $\mu t = 1{\cdot}5$ at 1 Å wavelength then the total power absorbed by the interferometer is reduced by a factor of around 30, whilst the intensity at 1 Å is only reduced by a factor of 5.

If we now set the interferometer to diffract 1 Å radiation, we have a situation in which we can use the thermal filter to control the power incident on the interferometer over a 30:1 range (at least), whilst still retaining enough intensity at 1 Å wavelength in the diffracted beam to record on film moiré images of the thermal strain distribution.

When a glass filter ($\mu t \simeq 0{\cdot}8$ at 1 Å) is placed in front of the wide-beam interferometer the thermal load on the interferometer is reduced by about 88% and the wider moiré fringes in Fig. 2(*b*) show that the temperature differential is decreased. For example, in the middle of the field of view the temperature differential is only 0·20 K compared with 1·39 K in Fig. 2(*a*). More important, the ratio of the fringe spacings at corresponding positions in the two parts of Fig. 2 is a constant showing that the temperature distribution is substantially independent of the beam power but scales with the power. The absorption power spectra for the interferometer beam splitter with and without the glass thermal filter are calculated in Fig. 4. The ratio of the areas under the absorption curves is about 8·5, in reasonable agreement with the measured temperature ratios. The discontinuities in the curve reflect the presence of heavy elements in the glass used in the experiments (4·5% Zn and 2·8% Pb). Further exposures with various thermal filters confirmed the result that the temperature rise accurately followed the calculated heat load in the beam splitter.

4. Control of thermal loading without filters

In order to make full use of the intensity of the synchrotron radiation source, it is preferable to avoid the use of filters in the beam. If we examine the geometric conditions necessary for the useful operation of a system similar to those successfully used in the laboratory (Cusatis & Hart, 1974, 1977; Siddons, 1979*a*,*b*; Hart & Siddons, 1978; Hart, 1980), then we find that for the proposed SRS at Daresbury, the minimum possible beam divergence in the vertical plane is of the order of 10^{-5} rad. This implies an optimum beam collimator dimension in this plane of 1 mm or less. It is thus interesting to study the effect of the size of the illuminated (and heated) region on the induced strain.

Fig. 5 shows a series of moiré topographs in which the total thermal loading was varied by a factor of 20 by changing the illuminated area from the original 9 × 6 mm to 0·4 × 6 mm. So that the fringes could be clearly resolved even with the largest beam, a thin thermal filter was used in front of the interferometer throughout this series of exposures.

Quantitative evaluation of these moiré patterns yields some interesting information, as Table 1 shows.

In each case the fringe spacing was measured at the centre of the field. The interesting result is that the temperature rise per unit beam area is *not* constant. Because the illuminated area is only part of a much larger wafer, the relative importance of the wafer as a heat sink increases as the beam area becomes smaller. The temperature rise is only half that which might have

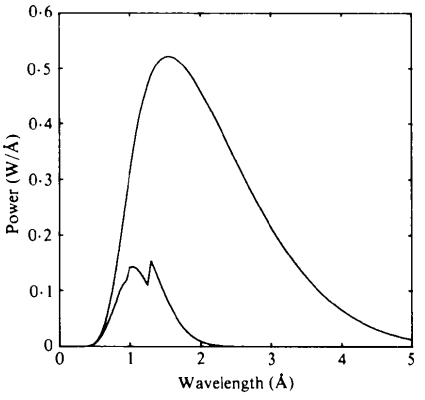

Fig. 4. Power spectrum of radiation absorbed in the beam splitter with and without the thermal filter under the conditions obtaining in Fig. 2. The discontinuities in the lower curve are due to transition metals (Pb and Zn) present in the glass.

been expected from a linear interpolation based upon a single measurement (such as the one in Fig. 2*a*) when the beam width is reduced to about 1 mm. Comparing the results in Figs. 5 and 2(*a*) we find that the filter factor in Fig. 5 (thermal) is 5·8. Thus, the results in Table 1 can be scaled by this factor to estimate the temperature rise with no filter. For a 0·5 × 6 mm beam, which might be used for high-resolution interferometric spectroscopy, the temperature rise would be only 0·04 K with no thermal filter. The corresponding moiré fringe spacing is 1·5 mm and this could easily be compensated with a wedge-shaped phase plate. Even if uncompensated the loss of contrast in a scanning interferometer would probably be tolerable so that monolithic scanning interferometers could be used directly in the white beam from either DCI or the SRS for dispersion spectroscopy at short wavelengths.

The analysis has been undertaken for other regions in the illuminated areas shown in Fig. 5. The bottom edge of each pattern is 5 mm above the base of the interferometer and the upper edge is defined by the second blade of the slit system which was used to control the total beam power. A quantitative analysis of the temperature distribution at the lower edge of the patterns, *i.e.* on a fixed line in the interferometer, again shows anomalously low temperatures when the beam is restricted by a narrow slit. From symmetry considerations, homogeneous strains over a ribbon beam could be obtained by choosing the shape of the interferometer wafer so as to equalize the thermal impedance of the portions of wafer above and below the slit.

Table 1. *Results of quantitative evaluation of moiré patterns*

Beam area	Fringe spacing	ΔT	ΔT/beam area
9 × 6 mm²	0·311 mm	0·241 K	0·45 ×10⁻² K mm⁻²
7 × 6	0·432	0·174	0·41
5 × 6	0·657	0·114	0·38
3·5 × 6	1·13	0·067	0·32
1·5 × 6	3·38	0·022	0·25
0·4 × 6	>6	<0·015	–

5. Two-dimensional heat flow

Table 1 shows the cooling which can be achieved when the beam is defined by a narrow slit. It is natural to ask whether an even greater effect can be obtained with pinhole collimation when two-dimensional heat flows are important. However, it is obviously not possible to observe large-spacing fringes within (say) a 1 mm diameter beam. It would be nice to image not only the heated area, but also its immediate surroundings in order to observe any strong strain gradients at the boundaries of the heated region. This condition may be achieved by making a small hole in our glass filter. The effect produced is shown in Fig. 6 where it is obvious that the 'hot spot' produced by the hole in the thermal filter has no effect on the details of the strain pattern produced; it serves simply to increase the local intensity incident on the interferometer. The strain inside the illuminated region does not reflect at all the spatial inhomogeneity of the thermal load placed upon it. The

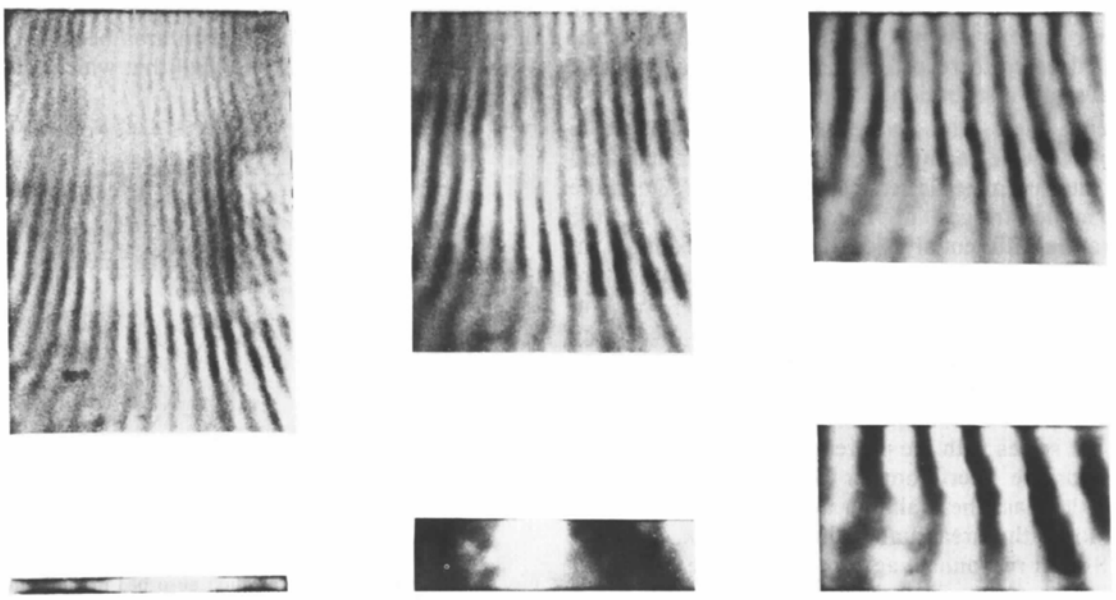

Fig. 5. Moiré topographs showing predominantly dilational strains obtained with various beam areas as listed in Table 1. 220 Bragg reflection at 1 Å wavelength; exposure time 15 s.

apparent shape of the pinhole results from severe over-exposure of the fringe which passes through the image. Its true shape can be seen in the pinhole image on the left-hand side of Fig. 6, which is a non-interfering beam from the interferometer.

6. Conclusions

We have directly measured the temperature distribution caused by beam heating in an X-ray interferometer. The quantitative results apply not only to interferometers but also to any silicon optical system.

In practice the effects of beam heating can be controlled, either by appropriate filtration when $\lambda < \lambda_{max}$ or by using small beams. The techniques of elastic design are well established in Bragg reflection X-ray optics and we must now concentrate simultaneously on aspects of good thermal design. For example, parts of a crystal system can be made to achieve homogeneous temperatures if appropriate thermal constrictions are cut into the wafers and their supporting structures.

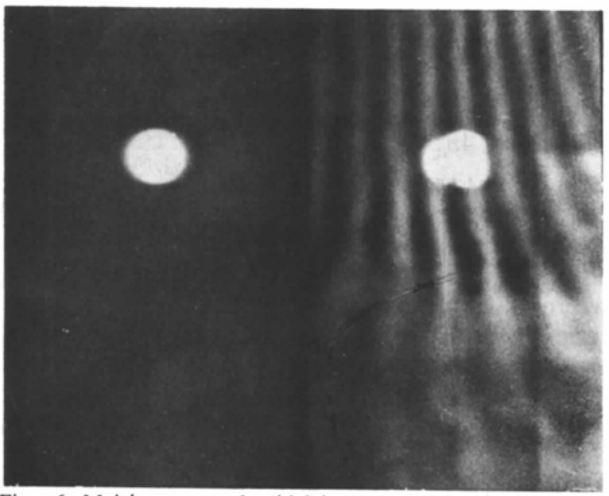

Fig. 6. Moiré topograph (right) and non-interfering beam topograph (left) showing the influence of a pinhole in the glass thermal filter. 220 Bragg reflection at 1 Å wavelength; field 11 × 6 mm; exposure time 30 s.

It would seem, from the preceding results, that, for the beam geometries demanded by high-resolution spectroscopy, silicon interferometers may be successfully used in the direct beam without special precautions.

Time constants for thermal equilibrium are also of practical interest. We obtained *identical* moiré patterns in a 15 s exposure on fast X-ray film and in a 4 min exposure on slow X-ray film. It follows that the time constant for thermal equilibration cannot be longer than a few seconds. In general, we can say that X-ray optical systems constructed of silicon should achieve thermal equilibrium in a few seconds. Any dynamic behaviour having longer time constants than this must be caused by parts of the X-ray optical system such as the crystal mount rather than by the crystal itself.

The authors are grateful to the staff of the Laboratoire de l'Accélérateur Linéaire for their help in these experiments. This work was supported by the Science Research Council.

References

ALDRED, P. J. E. (1970). PhD Thesis, Univ. of Bristol, England.

BONSE, U. & MATERLIK, G. (1976). *Z. Phys.* B**24**, 189–191.

BONSE, U., SPIEKER, P., HEIN, J.-T. & MATERLIK, G. (1979). National Conference on Synchrotron Radiation Instrumentation, NBS, Gaithersburg, USA.

CUSATIS, C. & HART, M. (1974). *Anomalous Scattering*. Copenhagen: Munksgaard.

CUSATIS, C. & HART, M. (1977). *Proc. R. Soc. London Ser. A*, **354**, 291–302.

HART, M. (1980). *Nucl. Instrum. Methods*, **172**, 209–214.

HART, M. & SIDDONS, D. P. (1978). *Proceedings of the First International Workshop on Neutron Interferometry*, Grenoble. Oxford Univ. Press.

International Tables for X-ray Crystallography (1968). Vol. III, 2nd ed. Birmingham: Kynoch Press.

SCHWINGER, J. (1949). *Phys. Rev.* **75**, 1912–1925.

SIDDONS, D. P. (1979*a*). PhD Thesis, Univ. of London, England.

SIDDONS, D. P. (1979*b*). *Bull. Inst. Phys.* pp. 105–106.